3D-QSAR Studies of 3,5-disubstituted Quinolines Inhibitors of c-Jun N-terminal Kinase-3

Thirumurthy Madhavan[†]

Abstract

c-Jun N-terminal kinase-3 (JNK-3) has been shown to mediate neuronal apoptosis and make the promising therapeutic target for neurodegenerative diseases such as Parkinson's disease, Alzheimer's disease, and other CNS disorders. In order to better understand the structural and chemical features of JNK-3, comparative molecular field analysis (CoMFA) was performed on a series of 3,5-disubstituted quinolines derivatives. The best predictions were obtained CoMFA model (q^2=0.707, r^2=0.972) and the statistical parameters from the generated 3D-QSAR models were indicated that the data are well fitted and have high predictive ability. The resulting contour map from 3D-QSAR models might be helpful to design novel and more potent JNK3 derivatives.

Key words : 3D-QSAR, CoMFA, JNK3

1. Introduction

c-Jun N-terminal Kinase (JNK) are serine threonine protein kinases and members of the mitogen activated protein kinase family (MAPK)[1-3]. JNK is activated by the dual phosphorylation of the motif Thr-Pro-Tyr located in the activation loop. JNK inactivation can be mediated by serine and tyrosine phosphotases[4]. JNK activate number of targets including members of the activator protein-1 family (AP-1), JunD, c-Jun, Bcl-2 proteins, c-Myc, activating transcriptional factor 2 (ATF2), and p53[5]. JNK proteins are encoded by three genes, JNK1, JNK2 and JNK3 and at least 10 different splicing isoforms exist in mammalian cells. JNK1 and JNK2 are widely expressed in tissues whereas JNK3 is selectively expressed in brain, heart and to lesser extent to testis[6,7]. JNK1 plays a key role in linking insulin resistance and obesity and JNK2 plays an important role in autoimmune and inflammatory diseases[8]. JNK3 has been shown to mediate neuronal apoptosis and make inhibiting this isoform a promising therapeutic target for neurodegenerative diseases such as Parkinson's disease,

Alzheimer's disease, and other CNS disorders[9-11]. Therefore, identifying JNK3 inhibitor may contribute towards neuroprotection therapies with reduced side effect risks, and will aid in further understanding of the roles of individual JNK kinases.

X-ray crystal structures of all three JNK isoforms have been reported. The overall architecture of JNKs is highly similar to that of other MAP kinases ERK2 and p38, consisting of an N-terminal domain with mostly β strands, a predominantly R helical C-terminal domain, and a deep cleft between N and C domains that comprises the ATP-binding site. The amino acid sequence identity of the JNK kinases is greater than 90% with >98% homology within the ATP binding site. High homology of the ATP-binding site among JNK's makes it challenging to design isoform specific ATP-site directed inhibitors. Therefore, designing selective ATP competitive JNK (1, 2, and 3) inhibitors is still a challenging task and the recent perspective by Siddiqui and Reddy stressed the importance of selectivity[12]. As selectivity is the major issue, our insilico analysis might be the starting point for the synthesis of highly potent and selective JNK3 analogs and this prompted us to initiate the analysis. The main aim of our study is to optimize the reported selective JNK3 inhibitors (3,5-disubstituted quinolines)[13] by Jiang and coworkers using the 3D-QSAR methodologies. We have per-

formed three dimensional quantitative structure activity relationship (3D-QSAR) using the comparative molecular field analysis (CoMFA)[14] techniques for JNK3 inhibitors to find the common structural features among them. The present work deals ligand-based technique based on the atom-by atom matching to generate reliable 3D-QSAR models. We expect that our theoretical results give some useful reference for the experimentalists in the design of novel and more potent JNK3 inhibitors.

2. Computational Methods
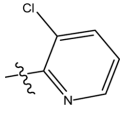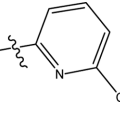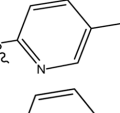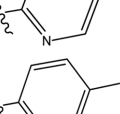
2.1. Inhibitor Data Set
The structures of the 4-anilinopyrimidines derivatives
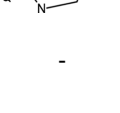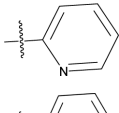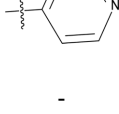
and their biological activities of thirty five compounds were taken from the literature[13]. All original IC_{50} value of each inhibitor was converted into pIC_{50} ($-logIC_{50}$) in order to use the data as dependent variable in CoMFA model. The test set molecule is truly representative molecule for training set molecules. The test set molecule should cover all the biological activity which is similar to the training set molecule. The total set of compounds was divided into a training set consist of 18 compounds and test set consist of 6 compounds. The selection of training and test sets were done manually so that low, moderate, and high JNK inhibitory activities were all represented. The structures and their activity values are displayed in Table 1.
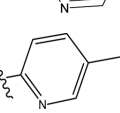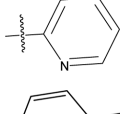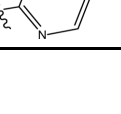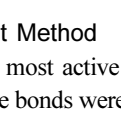
Table 1. Structures and biological activities (pIC50) of JNK3 inhibitors

| 1-9 | 10-18 | 19-20 | 21-22 | 23-24 |

Compound	R1	R2	R3	pIC50		Residual Value
				Actual	Predicted	
1	OH	-	-	6.229	5.909	0.320
2	H	-	-	6.000	6.291	-0.291
3*	5-Pyrazolyl	-	-	5.444	6.290	-0.846
4	Morpholino	-	-	5.886	5.880	0.006
5	NH$_2$	-	-	6.292	6.248	0.044
6	NAc$_2$	-	-	5.796	5.802	-0.006
7	NHAc	-	-	6.276	6.331	-0.055
8	NHMs	-	-	6.032	6.088	-0.056
9	NMS$_2$	-	-	6.678	6.652	0.026
10	-		-	6.357	6.319	0.038
11	-		-	6.319	6.344	-0.025
12	-		-	5.444	5.305	0.139
13*	-		-	6.119	6.271	-0.152

Table 1. Continued

Compound	R1	R2	R3	pIC50		Residual Value
				Actual	Predicted	
14	-		-	4.824	4.805	0.019
15	-		-	5.187	5.187	0.000
16	-		-	6.921	7.012	-0.091
17*	-		-	6.854	6.935	-0.081
18*	-		-	6.310	6.808	-0.498
19	-	-		5.284	5.542	-0.258
20	-	-		6.432	6.283	0.149
21*	-		-	6.824	6.676	0.148
22*	-		-	6.602	6.345	0.257
23	-		-	6.699	6.647	0.052
24	-		-	6.620	6.631	-0.011

*Test set compounds

2.2. Ligand-based Alignment Method

In ligand based alignment, the most active molecule was used as template. All rotatable bonds were searched with incremental dihedral angle from 120° by using systematic search conformation method. Conformational energies were computed with electrostatic term, and the lowest energy conformer was selected as template molecule. Then the template was modified for other ligands of the series. The common moiety was constraint for each molecule and only the varying parts were energy minimized by Tripos force field with Gasteiger-Huckel charge by using conjugate gradient method, and convergence criterion was 0.05 kcal/mol at 10,000 iteration. The minimized structures were aligned over template using atom fit option in Sybyl and subsequently this alignment is used for CoMFA analysis. The aligned molecules are represented in Figure 1.
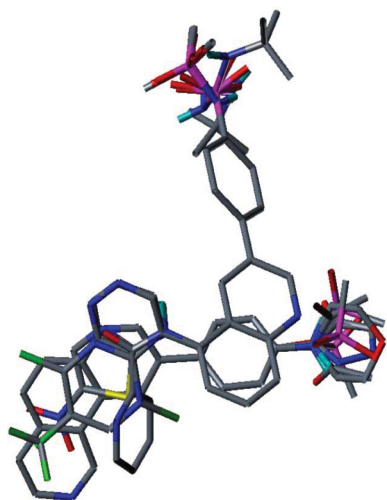
Fig. 1. Alignment of all molecules using atom-by-atom matching.

2.3. Generation of CoMFA and CoMSIA Field

Sybyl8.1 molecular modeling package is used in this study (15). CoMFA calculations were carried out by applying the default settings. The aligned molecules were placed in 3D cubic lattice with grid spacing of 1.0-2.0Å. The standard CoMFA field performing the Lennard-Jones potential and Coulombic potential for the steric and electrostatic fields respectively. A cut off value for both fields was set to 30 kcal/mol. Steric and electrostatic energies were calculated using sp^3 carbon atom with van der waals radius of 1.52Å and +1 charge at each lattice point.

2.4. Partial Least Square (PLS) Analysis

The relationship between the structural parameters and the biological activities has been quantified by the

PLS algorithm[16,17]. CoMFA and CoMSIA descriptors used as independent variables and pIC_{50} values used as dependent variables in PLS analysis for the generation of 3D-QSAR models. To select the best model, the cross-validation procedure was performed using leave one out (LOO) method, in this procedure one compound was removed from the data set and its activity was predicted using the model build from rest of the data set. It gives cross-validation correlation coefficient (q^2) and the optimum number of components. Final analyses i.e. non-cross-validation was performed to calculate conventional r^2_{ncv} using optimum number of components obtained from cross validation method. The cross-validated coefficient, q^2 is calculated using below Equation1.

$$q^2 = 1 - \frac{\sum(Y_{predicted} - Y_{observed})^2}{\sum(Y_{observed} - Y_{mean})^2} \qquad (1)$$

$Y_{predicted}$, $Y_{observed}$, and Y_{mean} are predicted, actual, and mean values of the target property (pIC_{50}), respectively. $\Sigma(Y_{predicted} - Y_{observed})^2$ is the predictive sum of squares (PRESS) and the lowest PRESS value is used to derive the final PLS models.

3. Results and Discussion

3.1. CoMFA Analysis

The optimum CoMFA model was derived with the combination of steric and electrostatic field contribution and Gasteiger-Hückel charge method with 2.0 Å grid space. The Leave one out (LOO) analysis gave the cross-validated q^2 of 0.707 with four components and noncross-validated PLS analysis resulted in a correlation coefficient r^2 of 0.972, F= 113.847, and an esti-

Table 2. Statistical summary of CoMFA models

CoMFA Models	Grid spacing (Å)	Leave-one-out cross-validation			Non-cross-validation			Bootstrap		r^2_{pred}	Field contribution	
		q^2	N	SDEP	r^2	SEE	F-value	r^2_{boot}	StdDev		S	E
(1)	1.0	0.690	4	0.522	0.973	0.153	119.088	0.986	0.011	-	0.554	0.446
(2)	1.5	0.685	4	0.526	0.972	0.156	114.196	0.980	0.012	-	0.564	0.436
(3)[a]	2.0	0.707	4	0.507	0.972	0.156	113.847	0.982	0.016	0.883	0.550	0.450

q^2= cross-validated correlation coefficient; N= number of statistical components; r^2= non-cross validated correlation coefficient; SEE= standard estimated error; F= Fisher value; r^2_{boot}= correlation coefficient after 100 runs of bootstrapping; $r^2_{predictive}$= predictive correlation coefficient for test set; S= steric; E= electrostatic; [a]The model chosen for CoMFA analysis is highlighted in bold font.
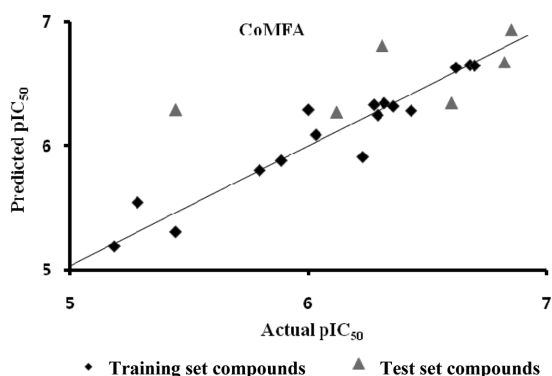
Fig. 2. Plot of actual versus predicted pIC_{50} values of the training set and test set compounds.
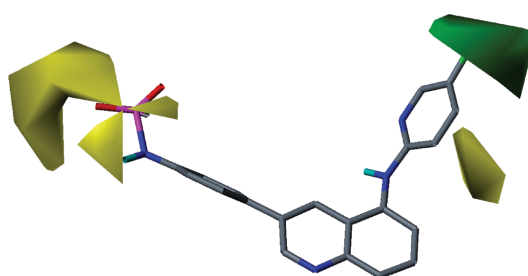

Fig. 3. CoMFA contour maps for steric field with highly active compound 16, where green contour indicates regions where bulky groups increases activity and yellow contours indicates bulky groups decreases activity.
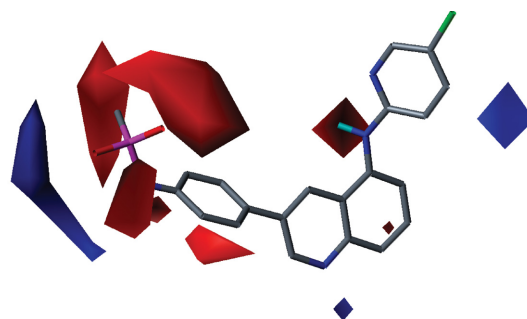

Fig. 4. CoMFA contour maps for electrostatic field with highly active compound 16, where blue contour indicates regions where electropositive groups increases activity and red contours indicates regions where electronegative groups increases activity

mated standard error of 0.156. We further performed bootstrapping analyses to evaluate the robustness and statistical confidence of the final models (r^2_{boot}=0.982, StdDev=0.016). Statistical results obtained from the constructed model verified the predictive ability of the model (Table 2) and further implied that the steric and electrostatic factors contribute to the binding affinities. The predictive ability of the developed CoMFA model was assessed by the test set (six molecules) predictions, which were excluded during CoMFA model generation. The predictive ability of the test set was 0.883. Predicted and experimental activities and their residual values of all inhibitors are shown in Table 1, and the corresponding scatter plot is depicted in Figure 2.

3.2. CoMFA Contour Map

The CoMFA contour map was generated based on the ligand-based (atom-by atom matching) alignment method. The CoMFA result is usually represented as 3D 'coefficient contour' map. It shows regions where variations of steric and electrostatic nature in the structural features of the different molecules contained in the training set lead to increase or decrease in the activity. The steric interaction is represented by green and yellow contours, in which green colored regions indicate areas where increased steric bulk is associated with enhanced activity, and yellow regions suggest areas where increased steric bulk is unfavorable to activity. The steric contour map is displayed in Figure 3. The green steric contour near the R_2 position of the phenyl ring indicates that bulkier substituent is preferred at this position. Thus, compounds 10-18 with bulkier substituent at this posi-

tion are more active. There was a yellow contour region was observed near to the R_1 position, the contour map indicated that substitution of bulkier groups would decrease the activity. This may be the reason that compounds 3, and 4 having bulkier substitution shows less activity. The electrostatic interaction is represented by red and blue contours (Figure 4), among which blue colored regions show areas where more positively charged groups are favored, and red region highlight areas where groups with more negative charges are favored. These contour maps give us some general insight into the nature of the receptor-ligand binding region. The electrostatic contour plot on the set of 24 compounds shows that there is a big red colored region situated close to the R_1 positions. The negative charges in these regions are very important for ligand binding, and electro negative group linked to this position will enhance the biological activity. For example, com-

pounds 9 having sulfonamide moiety shows more biological activity than other compounds[1-8].

4. Conclusion

In the present study, we developed satisfactory 3D-QSAR models of 3,5-disubstituted quinolines derivatives using CoMFA method based on the atom-by-atom matching alignment. The 3D-QSAR results revealed some important sites, such as steric, electrostatic modifications should significantly affect the bioactivities of the compounds. The steric contour map indicated that substitution of bulkier groups in the R_2 position of the phenyl ring would enhance the biological activity. Furthermore, the electrostatic contour map shows the important of hydrogen bond acceptor substitution in the R1 position. The information's have gathered from CoMFA studies demonstrated the way to understand the structural and chemical features of 3,5-disubstituted quinolines derivatives in designing and finding new potential JNK3 inhibitors.

References

[1] J. M. Kyriakis, and J.Avruch, "Pp54 microtubule-associated protein 2 kinase", J. Biol. Chem., Vol. 265, pp. 17355–17363, 1990.

[2] M. Hibi, A. Lin, T. Smeal, A. Minden, and M. Karin, "Identification of an oncoprotein and UVresponsive protein kinase that binds and potentiates the c-Jun activation domain", Genes and Development., Vol. 7, pp. 2135-2148, 1993.

[3] V. Adler, A. Polotskaya, F. Wagner, and A. S. Kraft, "Affinity-purified c-Jun amino-terminal protein kinase requires serine/threonine phosphorylation for activity", J. Biol. Chem., Vol. 267, pp. 17001-17005, 1992.

[4] R. J. Davis, "Signal transduction by the JNK group of MAP kinases", Cell., Vol. 103, pp. 239-252, 2000.

[5] A. M. Bode, and Z. Dong, "The functional contrariety of JNK", Molecular carcinogenesis., Vol. 46, pp. 591-598, 2007.

[6] S. Gupta, T. Barrett, A. J. Whitmarsh, J. Cavanagh, H. K. Sluss, B. Derijard, and R. J. Davis, " Selective interaction of JNK protein kinase isoforms with transcription factors", The EMBO Journal., Vol. 15, pp. 2760-2770, 1996.

[7] M. A. Bogoyevitch, "The isoform-specific functions of the c- Jun N-terminal kinases (JNKs): differences revealed by gene targeting", Bioessays., Vol. 28, pp. 923-934, 2006.

[8] J. H. Martin, A. A. Mohit, and C. A. Miller, "Developmental expression in the mouse nervous system of the p493F12 SAP kinase", Mol. Brain Res., Vol. 35, pp. 47-57, 1996.

[9] C. Dong, D.D. Yang, M. Wysk, A. J. Whitmarsh, R. J. Davis, and R. A. Flavell, "Defective T cell differentiation in the absence of Jnk1", Science., Vol. 282, pp. 2092-2095, 1998.

[10] J. M. Kyriakis, and J. Avruch, "Mammalian mitogen-activated protein kinase signal transduction pathways activated by stress and inflammation", Physiol. Rev., Vol. 81, pp. 807-869, 2001.

[11] G. Y. Zhang, and Q. G. Zhang, "Agents targeting c-Jun N-terminal kinase pathway as potential neuroprotectants", Expert Opin. Invest. Drugs., Vol. 14, pp. 1373-1383, 2005.

[12] J. M. A. Siddiqui and P. A. Reddy, "Small Molecule JNK (c-Jun N-Terminal Kinase) Inhibitors", J. Med. Chem., Vol. 53, pp. 3005-3012, 2010.

[13] R. Jiang, D. Duckett, W. Chen, J. Habel, Y. Y. Ling, P. L. Grassob, and T. M. Kamenecka, "3,5-Disubstituted quinolines as novel c-Jun N-terminal kinase inhibitors", Bioorganic and Medicinal Chemistry Letters., Vol. 17, pp. 6378-6382, 2007.

[14] R. D. Cramer, D. E. Patterson, and J. D. Bunce, "Comparative molecular field analysis (CoMFA).1. Effect of shape on binding of steroids to carrier proteins", J. Am. Chem. Soc., Vol. 110, pp. 5959–5967, 1988.

[15] Sybyl 8.1, Tripos Inc., St. Louis, MO 63144, USA.

[16] S. J. Cho, and A. Tropsha, "Cross-validated R2-guided region selection for comparative molecular field analysis: A simple method to achieve consistent results", J. Med. Chem., Vol. 38, pp.1060-1066, 1995.

[17] S. Wold, M. Sjostrom, and L. Eriksson, "PLS-regression: a basic tool of chemometrics", Chemometrics and intell. lab. Sy., Vol. 58, pp. 109-130, 2001.